

Nanometer Distance Measurements on RNA Using PELDOR

Olav Schiemann,^{*,†} Axel Weber,[†] Thomas E. Edwards,[‡] Thomas F. Prisner,[†] and Snorri T. Sigurdsson^{*,‡}

Institut für Physikalische und Theoretische Chemie, J. W. Goethe-Universität, Marie-Curie-Strasse 11, 60439 Frankfurt am Main, Germany, and Department of Chemistry, University of Washington, Seattle, Washington 98195-1700

Received June 26, 2002; E-mail: o.schiemann@prisner.de; snorrissi@hi.is

In addition to the transfer of genetic information to the site of protein synthesis, RNA also catalyzes chemical reactions.¹ Insights into the mechanism of RNA function can be obtained from structural studies. One highlight in this research area was the solution of a bacterial ribosome structure by X-ray crystallography.² Nevertheless, growing crystals and solving the structure of complex RNA molecules remains challenging. Therefore, spectroscopic methods, such as fluorescence resonance energy transfer measurements (FRET),³ nuclear magnetic resonance (NMR),⁴ and electron paramagnetic resonance (EPR),⁵ are useful for obtaining structural information in liquid or frozen solutions that resemble biological conditions.

EPR spectroscopy is a valuable technique for the determination of long-range distances in biopolymers using the dipolar coupling between unpaired electrons. Hence, information about the folded structure of RNA can be obtained by measuring the distance r_{AB} between spin labels that have been incorporated at known positions in the primary sequence. Modern pulsed EPR methods, such as pulsed electron double resonance (PELDOR, Scheme 1),⁶ have shown promise for measuring, with high precision, significantly longer distances⁷ than has previously been possible using continuous wave EPR.⁸ However, PELDOR measurements on spin-labeled molecules have only been applied to small organic molecules,⁹ polymers,¹⁰ or peptides¹¹ in nonaqueous solutions. Here we present the first example of using PELDOR for the determination of a distance exceeding 30 Å on a folded RNA biopolymer in an aqueous buffer solution.

PELDOR enables the measurement of the spin–spin coupling ν_{AB} (eq 1) between two unpaired electrons A and B in frozen solution by monitoring the echo amplitude Φ as a function of the position T of the inversion pulse between the $\pi/2$ - and π -pulse of the Hahn echo sequence. To suppress unwanted hyperfine coupling contributions, the $\pi/2$ – τ – π detection sequence is applied at a different microwave frequency than the inversion pulse. The echo amplitude oscillates with the frequency ν_{AB} , from which the distance r_{AB} can be calculated according to eqs 1 and 2,¹² where θ is the angle between the applied magnetic field B_0 and the electron distance vector r_{AB} ; J is the exchange coupling constant;¹³ μ_B is the Bohr magneton; μ_0 is the magnetic constant; h is the Planck constant; and g_A and g_B are the g -values of the unpaired electrons A and B, respectively. For spin–spin distances above 20 Å, the exchange coupling constant J is negligible,¹³ and the measured ν_{AB} contains only the distance dependent dipolar coupling constant ν_{Dip} and the orientation dependent factor $(1 - 3 \cos^2 \theta)$. The latter one can be determined from the same measurement if both singularities

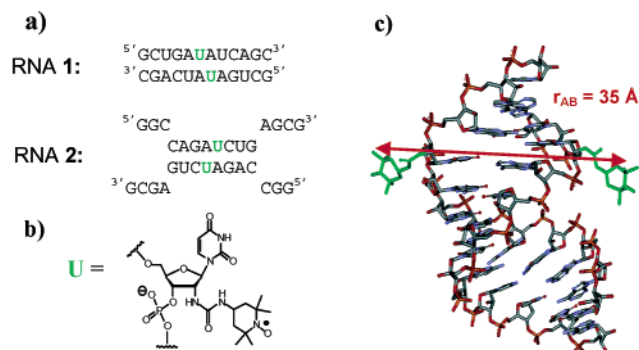
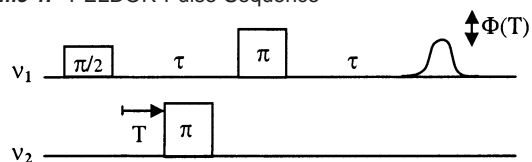


Figure 1. (a) Sequence of RNA 1 and 2. (b) The structure of the spin-labeled U. (c) Crystal structure of an A-form RNA with the two spin-labels attached using WebLab Viewer. The red arrow is the O–O distance r_{AB} between the nitroxides.

Scheme 1. PELDOR Pulse Sequence



of the Pake pattern at $\theta = 90^\circ$ and 0° are observed.¹⁴

$$\nu_{AB} = \nu_{Dip}(1 - 3 \cos^2 \theta) + J \quad (1)$$

$$\nu_{Dip} = \frac{\mu_B^2 g_A g_B \mu_0}{4\pi h} \cdot \frac{1}{r_{AB}^3} \quad (2)$$

We prepared the self-complementary RNA 1 (Figure 1a), containing spin-labeled uridines at the sequence 5'-UA·UA. Nitroxide spin-labels were conjugated to 2'-positions of the RNA with a urea linker (Figure 1b) by reaction of a 2'-amino group with a spin-labeled isocyanate.¹⁵ Optical melting experiments showed only a 1 °C lower melting temperature for the spin-labeled duplex, as compared with the unlabeled sequence. Modeling the spin-labels into a known RNA structure containing the 5'-UA·UA sequence¹⁶ (Figure 1c) yielded an O–O distance of 35 Å. For comparison, RNA 2 was prepared because it can populate different folds in solution, including a short duplex structure, and should thus yield a broad distance distribution.

The PELDOR spectra of RNA 1 and RNA 2 (Figure 2a, b) were recorded on an ELEXSYS e580 pulsed X-band EPR spectrometer extended by a second home-built pulsed microwave channel.¹⁴ The short T_2 relaxation times for RNA 1 and 2 (Supporting Information) restrict the choice of τ -values suitable for the PELDOR measurements to only 1.1 μ s and 520 ns, respectively. The echo decays

[†] University of Frankfurt.

[‡] University of Washington.

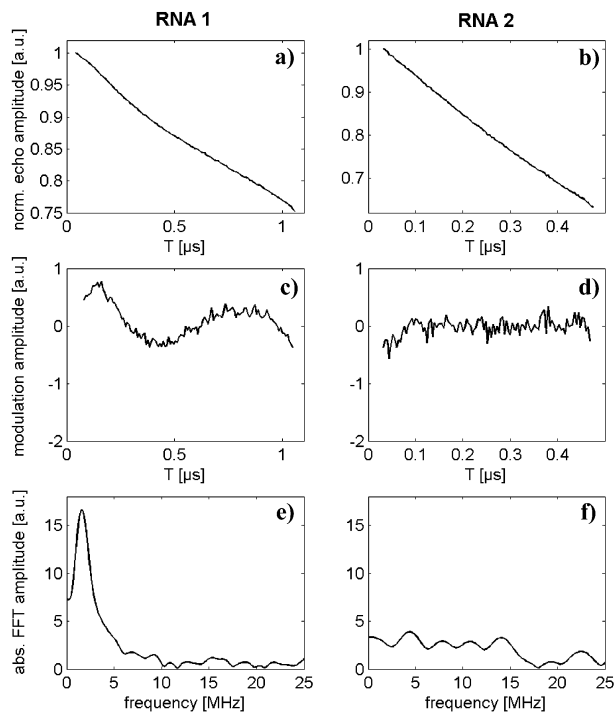


Figure 2. Time domain spectra before (a,b) and after subtracting the echo decay (c,d) and the frequency domain spectra (e,f) of RNA 1 and RNA 2 at 10 and 20 K, respectively. For the EPR measurements, both RNAs were dissolved in 80 μL of buffer (100 mM sodium chloride, 10 mM sodium phosphate, 0.1 mM Na_2EDTA , $\text{pH} = 7.2$) yielding final RNA concentrations of 0.3 mM.

seen in both PELDOR spectra, which are due to the coupling of A spins to randomly distributed B spins, were fitted exponentially and subtracted from the time domain spectra (Figure 2c, d). The result was Fourier transformed and yielded the frequency domain spectra shown in Figure 2e, f.

RNA 1 showed a low-frequency oscillation in the time domain, originating from the electron–electron coupling ν_{AB} (Figure 2a, c). After Fourier transformation, a peak at a frequency of 1.2 ± 0.2 MHz is readily observed (Figure 2e). This peak is assigned to the $\theta = 90^\circ$ orientation within Pake pattern, due to the weak orientation selection achieved by the position of the pulses with respect to the EPR field swept spectrum of the nitroxides.¹⁴ The contribution of the exchange coupling constant J to ν_{AB} of RNA 1 is negligible due to several σ - and hydrogen bonds between the two N–O groups.¹³ Thus, an r_{AB} of 35 ± 2 Å can be directly calculated using eq 2, in excellent agreement with the distance obtained from the model structure (Figure 1c). The weak modulation depth may be due to the flexibility of the linker used to attach the nitroxides to the RNA or to aggregation of the RNA duplexes.

Therefore, the degree of aggregation was estimated by calculating the average spin concentration of RNA 1 from the decay of the PELDOR echo, yielding 1.8 mM (Supporting Information).^{7,11} This is a factor of 3 larger than the nominal spin concentration of 0.6 mM, indicating that freezing the sample results in areas of concentrated RNA. Nevertheless, calculating from this concentration the average intermolecular spin–spin distances yields a value of 97 Å (Supporting Information), which is significantly larger than the intramolecular distance of 35 Å, demonstrating thereby the absence of aggregation for RNA 1.

In contrast to RNA 1, the PELDOR spectrum of RNA 2 (Figure 2b) shows neither a modulation of the echo amplitude nor a peak after Fourier transformation (Figure 2d, f). Furthermore, its time domain spectrum reveals a steep PELDOR echo decay which

corresponds to a strongly enlarged average spin concentration of 6.8 mM and an average intermolecular distance of 63 Å. This suggests some degree of aggregation for RNA 2, which could be rationalized by loop–loop or end–end interactions induced and promoted by the secondary structures of this RNA. To test whether the oscillation of RNA 1 would be visible under the aggregation conditions of RNA 2, we simulated a time domain spectrum with the oscillation of RNA 1 and the decay and time window of RNA 2. In this case also for RNA 1, no oscillation would be visible (Supporting Information). Consequently, aggregation and/or a weak population of duplex RNA 2 are the reasons for the lack of oscillation in its time domain spectrum.

In summary, in the absence of aggregation, PELDOR measurements yield precise intramolecular long-range distances under biologically relevant conditions. Application of this technique for the study of RNA tertiary structure in complex RNA folds is underway and will be reported in due course.

Acknowledgment. We thank the DFG (SFB 579), NIH (GM56947 and GM55963), and NIEHS for financial support. O.S. thanks the DFG for a Habilitation fellowship. T.E.E. was supported by the NIH National Research Service Award 5 T32 GM08268, and A.W. was supported by the DFG (SFB 472).

Supporting Information Available: Experimental parameters, calculations, simulations, EPR and ESEEM spectra (PDF). This material is available free of charge via the Internet at <http://pubs.acs.org>.

References

- (1) *The RNA World*, 2nd ed.; Gesteland, R. F., Cech, T. R., Atkins, J. F., Eds.; Cold Spring Harbor Laboratory Press: Cold Spring Harbor, 1999.
- (2) Ban, N.; Nissen, P.; Hansen, J.; Moore, P. B.; Steitz, T. A. *Science* **2000**, *289*, 905–930.
- (3) Walter, N. G.; Hampel, K. J.; Burke, J. M. *EMBO J.* **1998**, *17*, 2378–2391.
- (4) Richter, C.; Reif, B.; Griesinger, C.; Schwalbe, H. *J. Am. Chem. Soc.* **2000**, *122*, 12728–12731.
- (5) Prisner, T. F.; Rohrer, M.; MacMillan, F. *Annu. Rev. Phys. Chem.* **2001**, *52*, 279–313.
- (6) (a) Milov, A. D.; Salikhov, K. M.; Shirov, M. D. *Fiz. Tverd. Tela* **1981**, *23*, 975–982. (b) Milov, A. D.; Maryasov, A. G.; Tsvetkov, Y. D. *Appl. Magn. Reson.* **1998**, *15*, 107–143.
- (7) Jeschke, G. *Macromol. Rapid Commun.* **2002**, *23*, 227–246.
- (8) Eaton, S. S.; Eaton, G. R. In *Biological Magnetic Resonance*; Berliner, L. J., Eaton, S. S., Eaton, G. R., Eds.; Kluwer Academic/Plenum Publisher: New York, 2000; Vol. 19, p 8.
- (9) (a) Larsen, R. G.; Singel, D. J. *J. Chem. Phys.* **1993**, *98*, 5134–5146. (b) Martin, R. E.; Pannier, M.; Diederich, F.; Gramlich, V.; Hubrich, M.; Spiess, H. W. *Angew. Chem., Int. Ed.* **1998**, *37*, 2834–2837.
- (10) Pannier, M.; Schädler, V.; Schöps, M.; Wiesner, U.; Jeschke, G.; Spiess, H. W. *Macromolecules* **2000**, *33*, 7812–7818.
- (11) (a) Milov, A. D.; Tsvetkov, Y. D.; Formaggio, F.; Crisma, M.; Toniolo, C.; Raap, J. *J. Am. Chem. Soc.* **2001**, *123*, 3784–3789. (b) Codd, R.; Astashkin, A. V.; Pacheco, A.; Raitsimring, A. M.; Enemark, J. H. *J. Biol. Inorg. Chem.* **2002**, *7*, 338–350. (c) Persson, M.; Harbridge, J. R.; Hammarstrom, P.; Mitri, R.; Martensson, L.-G.; Carlsson, U.; Eaton, G. R.; Eaton, S. S. *Biophys. J.* **2001**, *80*, 2886.
- (12) Hustedt, E. J.; Beth, A. H. In *Biological Magnetic Resonance*; Berliner, L. J., Eaton, S. S., Eaton, G. R., Eds.; Kluwer Academic/Plenum Publisher: New York, 2000; Vol. 19, pp 155–184.
- (13) Kahn, O. *Molecular Magnetism*; VCH: New York, 1993.
- (14) Weber, A.; Schiemann, O.; Bode, B.; Prisner, T. F. *J. Magn. Reson.* **2002**, *157*, 277–285.
- (15) (a) Edwards, T. E.; Okonogi, T. M.; Robinson, B. H.; Sigurdsson, S. T. *J. Am. Chem. Soc.* **2001**, *123*, 1527–1528. (b) Edwards, T. E.; Okonogi, T. M.; Sigurdsson, S. T. *Chem. Biol.* **2002**, *9*, 699–706.
- (16) NDB-Atlas entry ARL062. Schindelin, H.; Zhang, M.; Bald, R.; Fuerste, J. P.; Erdmann, V. A.; Heinemann, U. *J. Mol. Biol.* **1995**, *249*, 595–603.

JA0274610